Functional analysis of the green fluorescent protein-tagged inositol 1,4,5-trisphosphate receptor type 3 in Ca^{2+} release and entry in DT40 B lymphocytes

Takao MORITA*, Akihiko TANIMURA*[1], Akihiro NEZU*, Tomohiro KUROSAKI†‡ and Yosuke TOJYO*

*Department of Dental Pharmacology, School of Dentistry, Health Sciences University of Hokkaido, Ishikari-Tobetsu, Hokkaido 061-0293, Japan, †Department of Molecular Genetics, Institute for Liver Research, Kansai Medical University, Moriguchi 570-8506, Japan, and ‡Laboratory for Lymphocyte Differentiation, RIKEN Research Center for Allergy and Immunology, Turumi-ku, Yokohama 230-0045, Japan

We examined the function of GFP-IP_3R3 (green fluorescent protein-tagged inositol 1,4,5-trisphosphate receptor type 3) in Ca^{2+} release and entry using a mutant DT40 cell line (IP_3R-KO) in which all three IP_3R genes had been disrupted. GFP-IP_3R3 fluorescence largely overlapped with the distribution of endoplasmic reticulum, whereas a portion of GFP-IP_3R3 apparently co-localized with the plasma membrane. The application of IP_3 to permeabilized WT (wild-type) DT40 cells induced Ca^{2+} release from internal stores. Although this did not occur in IP_3R-KO cells it was restored by expression of GFP-IP_3R3. In intact cells, application of anti-IgM, an activator of the BCR (B-cell receptor), or trypsin, a protease-activated receptor 2 agonist, did not cause any Ca^{2+} response in IP_3R-KO cells, whereas these treatments induced oscillatory or transient Ca^{2+} responses in GFP-IP_3R3-expressing IP_3R-KO cells, as well as in WT cells. In addition, BCR activation elicited Ca^{2+} entry in WT and GFP-IP_3R3-expressing IP_3R-KO cells but not in IP_3R-KO cells. This BCR-mediated Ca^{2+} entry was observed in the presence of La^{3+}, which blocks capacitative Ca^{2+} entry. Thapsigargin depleted Ca^{2+} stores and led to Ca^{2+} entry in IP_3R-KO cells irrespective of GFP-IP_3R3 expression. In contrast with BCR stimulation, thapsigargin-induced Ca^{2+} entry was completely blocked by La^{3+}, suggesting that the BCR-mediated Ca^{2+} entry pathway is distinct from the capacitative Ca^{2+} entry pathway. The present study demonstrates that GFP-IP_3R3 could compensate for native IP_3R in both IP_3-induced Ca^{2+} release and BCR-mediated Ca^{2+} entry.

Key words: Ca^{2+} entry, Ca^{2+} release, DT 40 cell, green fluorescent protein, imaging, inositol 1,4,5-trisphosphate receptor.

INTRODUCTION

The IP_3R (inositol 1,4,5-trisphosphate receptor) is an intracellular IP_3-induced Ca^{2+} release channel composed of an N-terminal cytoplasmic IP_3-binding domain and a C-terminal channel domain. In mammalian cells, there are at least three IP_3R subtypes, type 1 (IP_3R1), type 2 (IP_3R2) and type 3 (IP_3R3), which exhibit different tissue distributions [1,2].

Immunocytochemical and subcellular fractionation studies have demonstrated that IP_3Rs are distributed to Ca^{2+} storage organelles such as the ER (endoplasmic reticulum) and nuclear envelope [2]. It has also been reported that IP_3Rs localize to certain areas in some cell types. For example, in polarized epithelial cells, such as pancreatic acinar cells and salivary cells, the IP_3R is mainly localized to the apical pole, which corresponds to the trigger zone from which apical-to-basal Ca^{2+} waves originate [3–5]. Thus the subcellular localization of the IP_3R is considered to play an important part in determining the spatio-temporal characteristics of Ca^{2+} signals.

In addition to its distribution in intracellular organelles, there is also evidence indicating that a portion of the IP_3R is localized to, or is in close proximity to, the plasma membrane in a variety of cell types [6–10]. These IP_3Rs are considered to participate in Ca^{2+} entry across the plasma membrane [6,8,9,11]. Moreover, the results of several recent studies suggest that IP_3Rs migrate during cell growth and maturation [12,13].

Recently, GFP (green fluorescent protein) has been used as an expression tag to study targeting and dynamics of intracellular molecules. In a previous study, we constructed an expression vector for a fusion protein of GFP and the full-length rat IP_3R3 (GFP-IP_3R3) [14]. This enabled us to visualize the distribution of IP_3Rs in living cells, although we could not determine the function of GFP-IP_3R3 since this was hampered by the existence of native IP_3Rs. In the present study, we expressed GFP-IP_3R3 in a mutant DT40 cell line (IP_3R-KO), in which all three IP_3R genes had been disrupted by a homologous recombination [15]. Our results demonstrate that GFP-IP_3R3 acts as a functional IP_3-induced Ca^{2+} release channel. In addition, we provide strong evidence that IP_3Rs are required for BCR (B-cell receptor)-mediated Ca^{2+} entry in DT40 cells. Moreover, GFP-IP_3R3 is also effective at compensating for native IP_3R in BCR-mediated Ca^{2+} entry.

MATERIALS AND METHODS

Materials and media

Anti-chicken IgM (supernatant, M-4 clone) was from Southern Biotechnology Associates (Birmingham, AL, U.S.A.). Polyclonal anti-GFP was from Medical & Biological Laboratories (Nagoya, Japan). Peroxidase-conjugated goat anti-rabbit antibody was purchased from Pierce (Rockford, IL, U.S.A.). Rabbit polyclonal antibodies, termed ABsI, ABsII and ABsIII, were raised against

Abbreviations used: BCR, B-cell receptor; GFP, green fluorescent protein; EGFP, enhanced GFP; ER, endoplasmic reticulum; fura 2/AM, fura 2 acetoxymethyl ester; ICM, intracellular-like medium; IP_3, inositol 1,4,5-trisphosphate; IP_3R, IP_3 receptor; PAR, protease-activated receptor; PLC, phospholipase C; ThG, thapsigargin; TR-DHPE, Texas Red-1,2-dihexadecanoyl-*sn*-glycero-3-phosphoethanolamine; WT, wild-type.

[1] To whom correspondence should be addressed (email tanimura@hoku-iryo-u.ac.jp).

the C-termini of human IP_3R1, IP_3R2 and IP_3R3 respectively and were affinity-purified and shown to be type-specific [10].

Fura 2/AM (fura 2 acetoxymethyl ester) and mag-fura 2/AM were from Molecular Probes (Eugene, OR, U.S.A.). Poly-(L-lysine) was from Sigma (St. Louis, MO, U.S.A.). Cellmatrix I-C was from Nitta Gelatin (Osaka, Japan). Tosyl-L-phenylalanylchloromethylketone ('TPCK') was obtained from Roche (Basel, Switzerland). Soya bean trypsin inhibitor was from Sigma. PMSF, pepstatin A, leupeptin and dithiothreitol were from Wako Pure Chemicals (Osaka, Japan). Tris/glycine SDS sample buffer and 3–8 % NuPAGE Tris/acetate gels were from Novel Experimental Technology (San Diego, CA, U.S.A.). pEGFP-C3 plasmid (where EGFP stands for enhanced GFP) was purchased from Clontech Laboratories (Palo Alto, CA, U.S.A.).

Modified Hanks' balanced salt solution buffered with Hepes (HBSS-H) contained 137 mM NaCl, 5.4 mM KCl, 1.3 mM $CaCl_2$, 0.41 mM $MgSO_4$, 0.49 mM $MgCl_2$, 0.34 mM Na_2HPO_4, 0.44 mM NaH_2PO_4, 5.5 mM glucose and 20 mM Hepes/NaOH (pH 7.4). Nominally, Ca^{2+}-free HBSS-H was identical in composition except for the omission of added $CaCl_2$. Na_2HPO_4 and NaH_2PO_4 were omitted in phosphate anion-free HBSS-H.

ICM (intracellular-like medium) contained 125 mM KCl, 19 mM NaCl, 10 mM Hepes (pH 7.3 with KOH), 330 μM $CaCl_2$ and 1 mM *O*,*O*′-bis (2-aminoethyl) ethyleneglycol-*N*,*N*,*N*′-*N*′-tetraacetic acid (free Ca^{2+} concentration was 50 nM).

The homogenization buffer contained 93.5 mM trisodium citrate, 6.2 mM citrate, 200 μM PMSF, 10 μM pepstatin A, 100 μM tosyl-L-phenylalanylchloromethylketone, 1 mM dithiothreitol, 10 μM leupeptin and 0.1 mg/ml soya bean trypsin inhibitor.

Cell culture and transfections

The DT40 chicken B-cell line and triple IP_3R-deficient cell line were cultured in RPMI 1640 (Sigma), supplemented with 10 % (v/v) fetal bovine serum (Trace, Noble Park, Vic., Australia), 1 % chicken serum (Gibco BRL, Rockville, MD, U.S.A.), 4 mM glutamine (Gibco BRL), 50 μM 2-mercaptoethanol (Nakarai Chemicals, Kyoto, Japan), 100 units/ml penicillin and 100 μg/ml streptomycin (Gibco BRL).

Transient transfections were performed using LIPOFECTAMINE™ 2000 reagent (Invitrogen, Carlsbad, CA, U.S.A.) with 1.6 μg/ml of plasmid according to the manufacturer's instructions.

Stable transfections of HSY-EA1 cells with the GFP-IP_3R3 plasmid vector (pCB-EGFP:IP_3R3) [14] were established using LIPOFECTAMINE™ 2000 reagent. G418 (Gibco BRL) selection (0.4 mg/ml) was initiated 24 h after the transfection. After 1 week, cells were expanded for an additional week without G418. Colonies of GFP-IP_3R3-expressing cells were screened by fluorescence microscopy. Stably transfected HSY-EA1 cells of GFP-IP_3R3 were cultured in Dulbecco's modified Eagle's medium Nutrient Mixture F-12 HAM (Sigma) supplemented with 10 % (v/v) newborn calf serum (Gibco BRL), 100 units/ml penicillin and 100 μg/ml streptomycin. The A431 human carcinoma cell line was cultured in Dulbecco's modified Eagle's medium (Sigma) with high glucose (25 mM), supplemented with 10 % fetal bovine serum, 4 mM glutamine, 1 mM sodium pyruvate, 100 units/ml penicillin and 100 μg/ml streptomycin.

Imaging of $[Ca^{2+}]_i$ (cytosolic Ca^{2+} concentration) and $[Ca^{2+}]_L$ (Ca^{2+} concentrations within Ca^{2+} stores)

For monitoring of $[Ca^{2+}]_i$, cells were attached to a small recording chamber consisting of a 10 mm ring and 22 mm glass coverslips coated with 0.5 mg/ml poly(L-lysine) and Cellmatrix (diluted 1/10). Attached cells were incubated with culture medium for 1 h at 37 °C and loaded with 2 μM fura 2/AM in HBSS-H containing 1 % BSA for 30 min at room temperature (22 ± 3 °C). The fura 2-loaded cells were washed with HBSS-H and rested for at least 15 min before Ca^{2+} measurements. Cells were alternately excited at 340 and 380 nm, with emission signals being recorded at 500–530 nm. Fluorescence images of GFP were captured at an excitation wavelength of 490 nm and emission wavelength of 500–530 nm using the Argus-HiSCA imaging system (Hamamatsu photonics, Shizuoka, Japan) attached to an inverted fluorescence microscope, equipped with a Nikon Fluor 40× objective.

For $[Ca^{2+}]_L$ monitoring, cells were loaded with mag-fura 2 and permeabilized, essentially as described previously [16]. Briefly, cells were incubated with 8 μM mag-fura 2/AM in HBSS-H containing 1 % BSA for 45 min at 37 °C in the dark. The mag-fura 2-loaded cells were washed with BSA-free HBSS-H and attached to Cell-Tak (BD Biosciences, Bedford, MA, U.S.A.) coated glass coverslips at the bottom of the recording chambers. Attached cells were washed with ICM, followed by exposure to ICM containing 100 μg/ml (w/v) saponin (ICN, Cleveland, OH, U.S.A.) for 1–2 min. The permeabilized cells were washed with ICM and then incubated in ICM containing 3 mM ATP and 1.4 mM $MgCl_2$ for at least 5 min. Fluorescent images of mag-fura 2 were acquired with dual excitation at 343 and 380 nm and an emission wavelength of 500–530 nm using the Argus-HiSCA imaging system equipped with a Nikon UV-Fluor ×100 objective. All these experiments were performed at room temperature.

Evaluation of IP_3R activity

Mag-fura 2-loaded cells were permeabilized and incubated in ICM containing 3 mM ATP and 1.4 mM $MgCl_2$. The cells were then washed with Ca^{2+}-releasing medium, consisting of ICM with 497 μM $CaCl_2$ (free Ca^{2+} concentration was 100 nM), 5 mM ATP and no $MgCl_2$. After exposure to various concentrations of IP_3, 10 μM IP_3 was added to deplete Ca^{2+} stores at the end of the experiment. The time course of Ca^{2+} release was monitored by following the change in the fluorescence ratio of mag-fura 2, and the time taken for the fluorescence ratio to decrease by half the value at the depleted level was noted. The average rate of fluorescence change was used as an index of IP_3R activity.

Confocal microscopy

The employed multi-photon microscope system included a femtosecond, pulsed Ti:sapphire laser (Mai Tai from Spectra-Physics, Mountain View, CA, U.S.A.) and a confocal microscope (Radiance 2100; BioRad, Hemel Hempstead, Herts., U.K.) with a four-line argon-ion laser and a Green HeNe laser. The pulsed laser is optically pumped by a 5 W green diode laser and has an output wavelength tuning range from 780 to 920 nm, which provides the source for a two-photon excitation. A Nikon Plan Apo × 60 H objective (NA = 1.4) was used for imaging.

The GFP-IP_3R3-expressing cells were attached to poly(L-lysine)/Cellmatrix-coated chambers and were incubated with culture medium for 1 h at 37 °C. Cells were then stained with 100 nM ER-Tracker Blue-White DPX (Molecular Probes) or 50 μM TR-DHPE (Texas Red-1,2-dihexadecanoyl-*sn*-glycero-3-phosphoethanolamine; Molecular Probes) in HBSS-H containing 1 % BSA for 10–50 min at 37 °C.

GFP-IP_3R3 and TR-DHPE fluorescence were visualized using dual-excitation beams in a line sequential mode with the argon-ion laser at 488 nm (GFP-IP_3R3) and the Green HeNe laser at 542 nm (TR-DHPE) in combination with a 560DCLP dichroic mirror and two emission filters, 500LB and 570LP. ER-Tracker

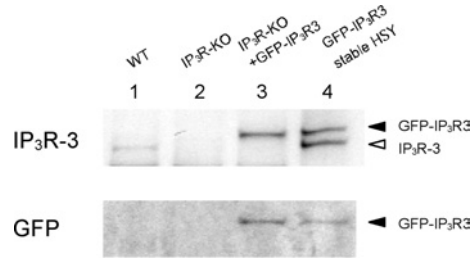

Figure 1 Expression of native IP_3R3 and GFP-IP_3R3

Microsomal fractions from WT DT40 cells (lane 1), IP_3R-KO cells (lane 2) and pCB-EGFP:IP_3R3-transfected IP_3R-KO cells (lane 3) (15 μg of protein/lane) and the membrane fraction from pCB-EGFP:IP_3R3 stably transfected HSY-EA1 cells (lane 4) (5 μg of protein/lane) were analysed by immunoblotting with ABsIII (upper panel) or anti-GFP (lower panel).

was excited by an 800 nm pulse laser and the emission signal was obtained using a 625SP blocking filter.

Preparation of protein extracts

DT40 cells grown in 100 mm culture dishes (Becton Dickinson, Franklin Lakes, NJ, U.S.A.) were washed with HBSS-H and were resuspended in 5 ml ice-cold homogenization buffer. These cells were disrupted with a Polytron homogenizer (2×20 s) and were centrifuged at 1500 ***g*** for 5 min. The supernatant was centrifuged (40000 ***g*** for 20 min at 4 °C), and the resulting microsomal pellet was resuspended in homogenization buffer and stored at − 80 °C until use. Preparation of the membrane fraction from stably transfected HSY-EA1 GFP-IP_3R3 cells was performed as described previously [14].

Western blotting

Samples were subjected to electrophoresis on 3–8 % NuPAGE Tris/acetate gels and transferred on to nitrocellulose membranes. For detection of IP_3Rs, transferred membranes were blocked with Block Ace (Dainippon Pharmaceuticals, Osaka, Japan) containing 10 % (v/v) goat serum, and were then incubated for 2 h with either ABsI, ABsII or ABsIII in 10 % Block Ace. For detection of GFP, transferred membranes were blocked with PBS containing 5 % (w/v) skimmed milk, 10 % goat serum and 0.05 % Tween 20, and then incubated for 1 h with PBS containing 5 % skimmed milk, 0.05 % Tween 20 and anti-GFP polyclonal antibody. These membranes were incubated for 1 h with peroxidase-conjugated goat anti-rabbit antibody in the 10 % Brock Ace containing 0.04 % Tween 20. Immunoreactive bands were visualized using the SuperSignal West Dura substrate (Pierce) and the intensity of chemiluminescence was measured using a Bio/Chemi-Luminescence imaging system (Light Capture, Atto, Tokyo, Japan).

RESULTS

GFP-IP_3R3 expression in IP_3R-KO DT40 cells

Figure 1 shows the expression of native type3 IP_3R and GFP-IP_3R3 in DT40 cells. In HSY-EA1 cells stably transfected with GFP-IP_3R3 (lane 4), anti-IP_3R3 recognized native IP_3R3 at approx. 260 kDa and GFP-IP_3R3 at approx. 275 kDa. Anti-GFP recognized only the approx. 275 kDa band, confirming that this upper band represents GFP-IP_3R3 (lane 4). WT (wild-type) DT40 cells (lane 1) expressed IP_3R3, whereas no signal was detected in IP_3R-KO cells (lane 2). After transient transfection of IP_3R-KO cells with the GFP-IP_3R3 plasmid, GFP-IP_3R3 expression was demonstrated with both anti-IP_3R3 and anti-GFP (lane 3).

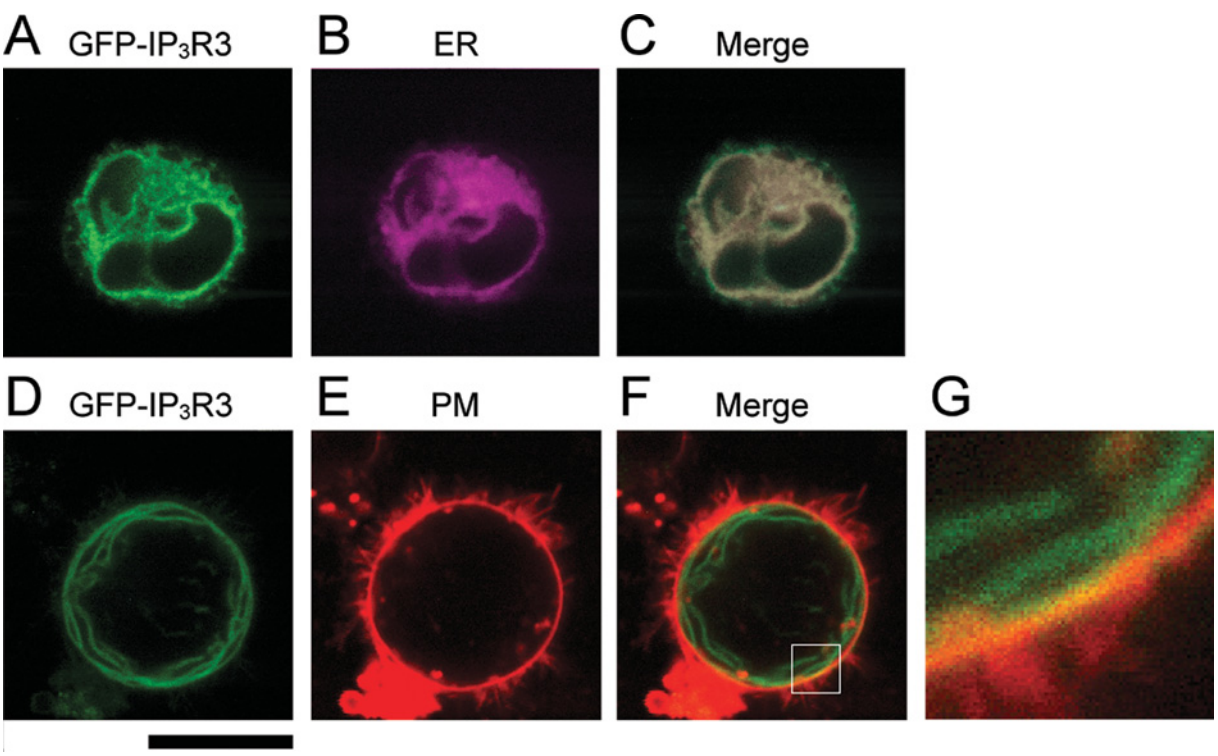

Figure 2 Subcellular localization of the GFP-IP_3R3 in IP_3R-KO DT40 cells

pCB-EGFP:IP_3R3-transfected IP_3R-KO cells were stained with ER-Tracker or TR-DHPE, and the fluorescence of GFP-IP_3R3 (**A**, **D**), ER-Tracker (**B**) and TR-DHPE (**E**) was visualized with a multi-photon microscope. (**C**) A merged view of (**A** and **B**). (**F**) A merged view of (**D** and **E**). (**G**) A higher magnification of the area indicated in (**F**). Scale bar, 10 μm.

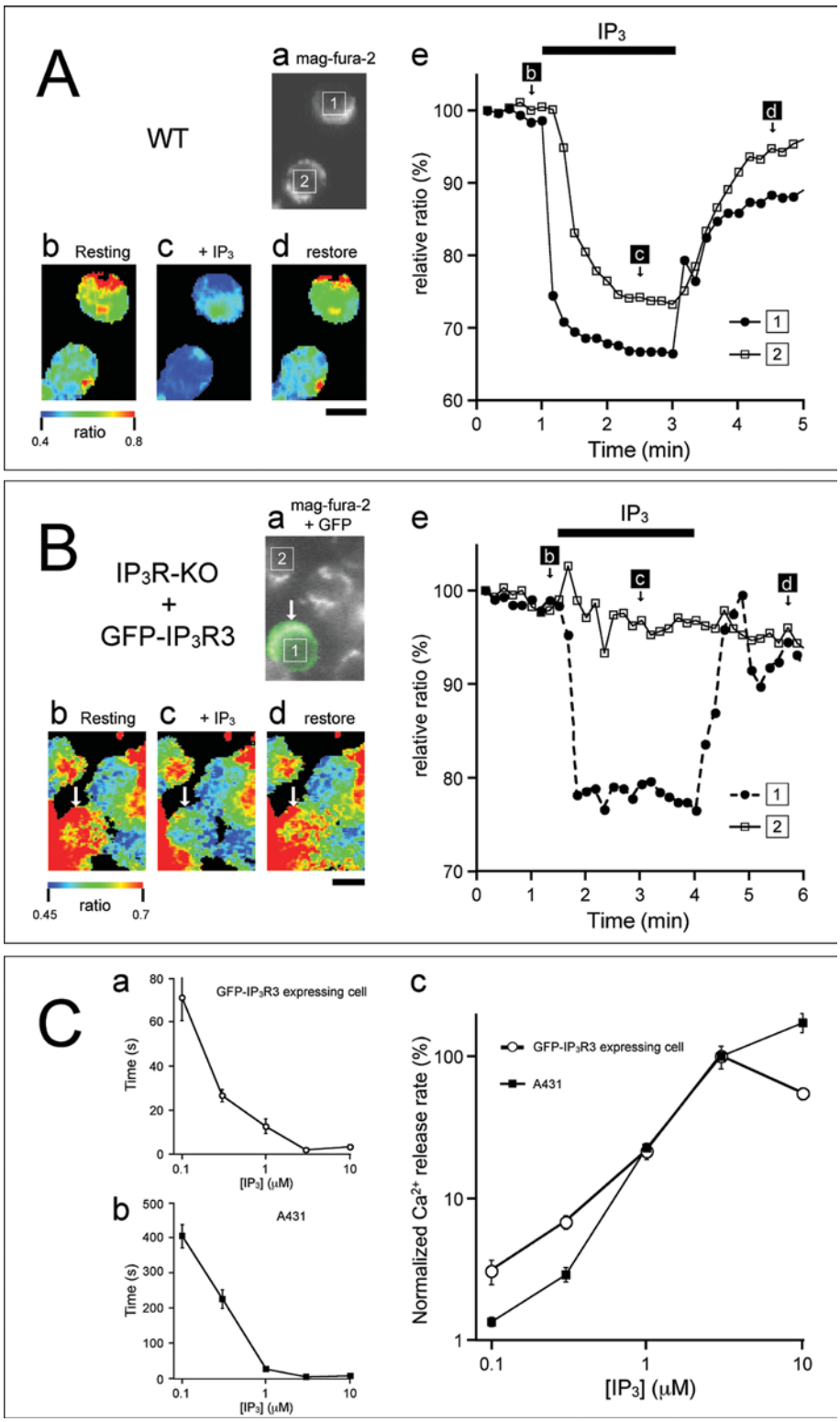

Figure 3 IP_3-induced Ca^{2+} release in saponin-permeabilized cells

WT DT40 (**A**) and GFP-IP_3R3-expressing IP_3R-KO DT40 (**B**) cells were loaded with mag-fura 2 and were permeabilized with saponin. Cells were then stimulated with IP_3 (1 μM) in ICM containing ATP and Mg^{2+}. (**A**) (a) Fluorescence image of mag-fura 2; (b–d) pseudocolour images of the mag-fura 2 ratio obtained at time points indicated in (e); (e) time-dependent changes as relative (%) fluorescence ratio in the cells depicted in the fluorescence image (a). (**B**) (a) Merged fluorescence image of GFP-IP_3R3 and mag-fura 2; (b–d) pseudocolour images of the mag-fura 2 ratio obtained at time points indicated in (e); (e) time-dependent changes as relative (%) fluorescence ratio in the cells depicted in the fluorescence image (a). The GFP-IP_3R3-expressing cell is indicated with an arrow. The horizontal bars at the top of the Figure indicate the presence of IP_3 in ICM. The ratio is presented as relative fluorescence intensity (F_{343}/F_{380}). Scale bar, 10 μm. (**C**) IP_3-concentration dependence of Ca^{2+} release for GFP-IP_3R3 and WT IP_3R3. Stable GFP-IP_3R3-expressing cells (a) and A431 cells (b) were permeabilized and exposed to various concentrations of IP_3 in ICM containing 100 nM free Ca^{2+}, 5 mM ATP and no $MgCl_2$. (a, b) Time taken for the fluorescence ratio to decrease by half the value at the depleted store level were plotted as a function of IP_3 concentration. (c) Normalized Ca^{2+} release rates at various IP_3 concentrations were compared between GFP-IP_3R3-expressing cells and A431 cells. Results are means $\pm$ S.E.M.

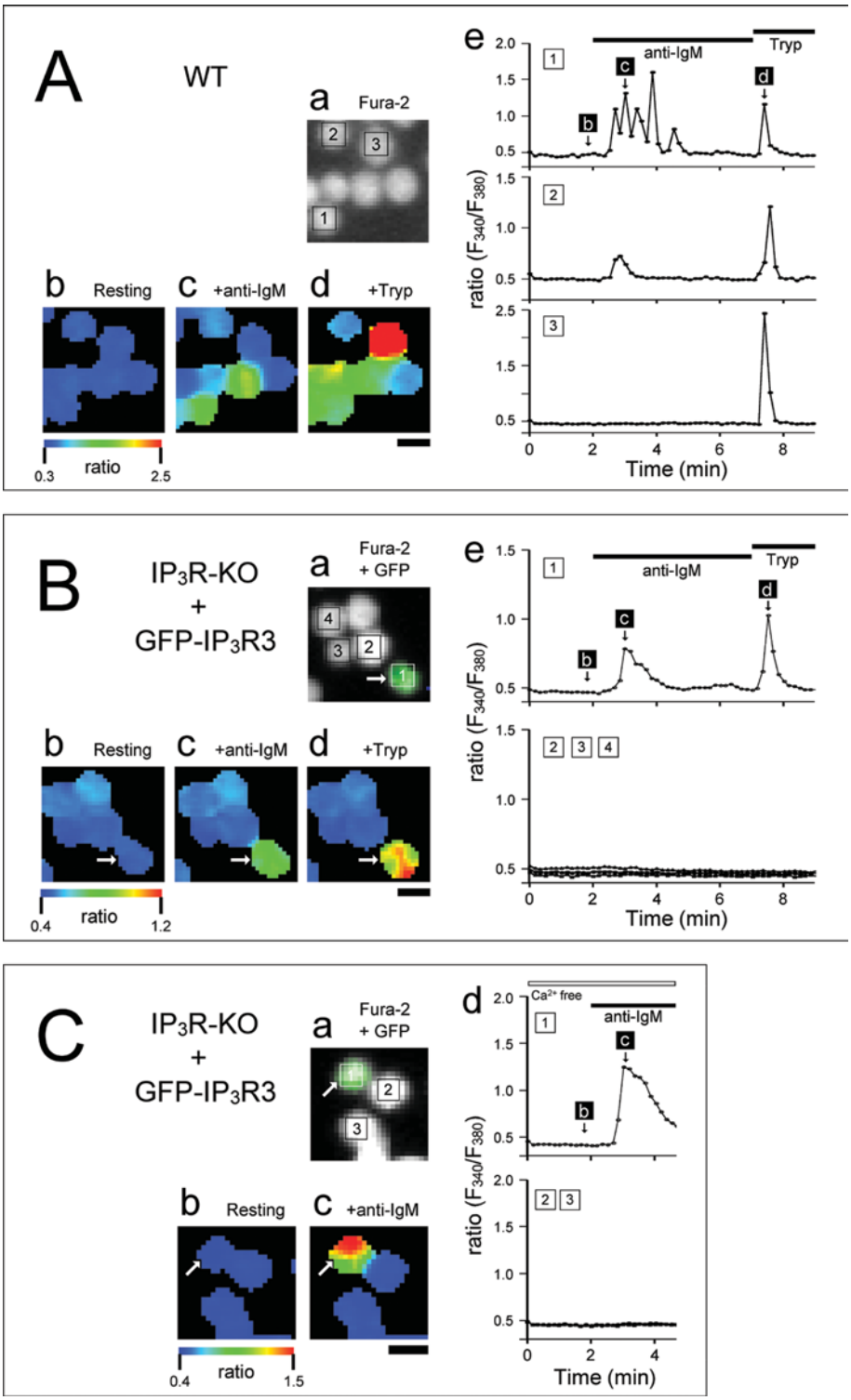

Figure 4 Agonist-induced Ca^{2+} responses in DT40 cells

WT (**A**) and GFP-IP_3R3-transfected IP_3R-KO (**B**, **C**) cells were stimulated with anti-IgM antibody (5 μg/ml) and trypsin (20 units/ml) in HBSS-H (**A**, **B**) or in nominally Ca^{2+}-free HBSS-H (**C**). (**A**) (a) Fluorescence image of fura 2; (b–d) pseudocolour images of the fura 2 ratio obtained at time points indicated in (e); (e) time-dependent changes in the fluorescence ratio in the cells depicted in (a). (**B**) (a) Merged fluorescence image of GFP-IP_3R3 and fura 2; (b–d) pseudocolour images of the fura 2 ratio obtained at time points indicated in (e); (e) time-dependent changes in the fluorescence ratio in the cells depicted in (a). GFP-IP_3R3-expressing cell is indicated by an arrow. (**C**) (a) Merged fluorescence image of GFP-IP_3R3 and fura 2; (b–c) pseudocolour images of the fura 2 ratio obtained at time points indicated in (d); (d) time-dependent changes in the fluorescence ratio in the cells depicted in (a). A GFP-IP_3R3-expressing cell is indicated by arrow. The horizontal bars at the top of the Figure indicate the presence of anti-IgM and trypsin. The ratio is presented as relative fluorescence intensity (F_{340}/F_{380}). Scale bar, 10 μm.

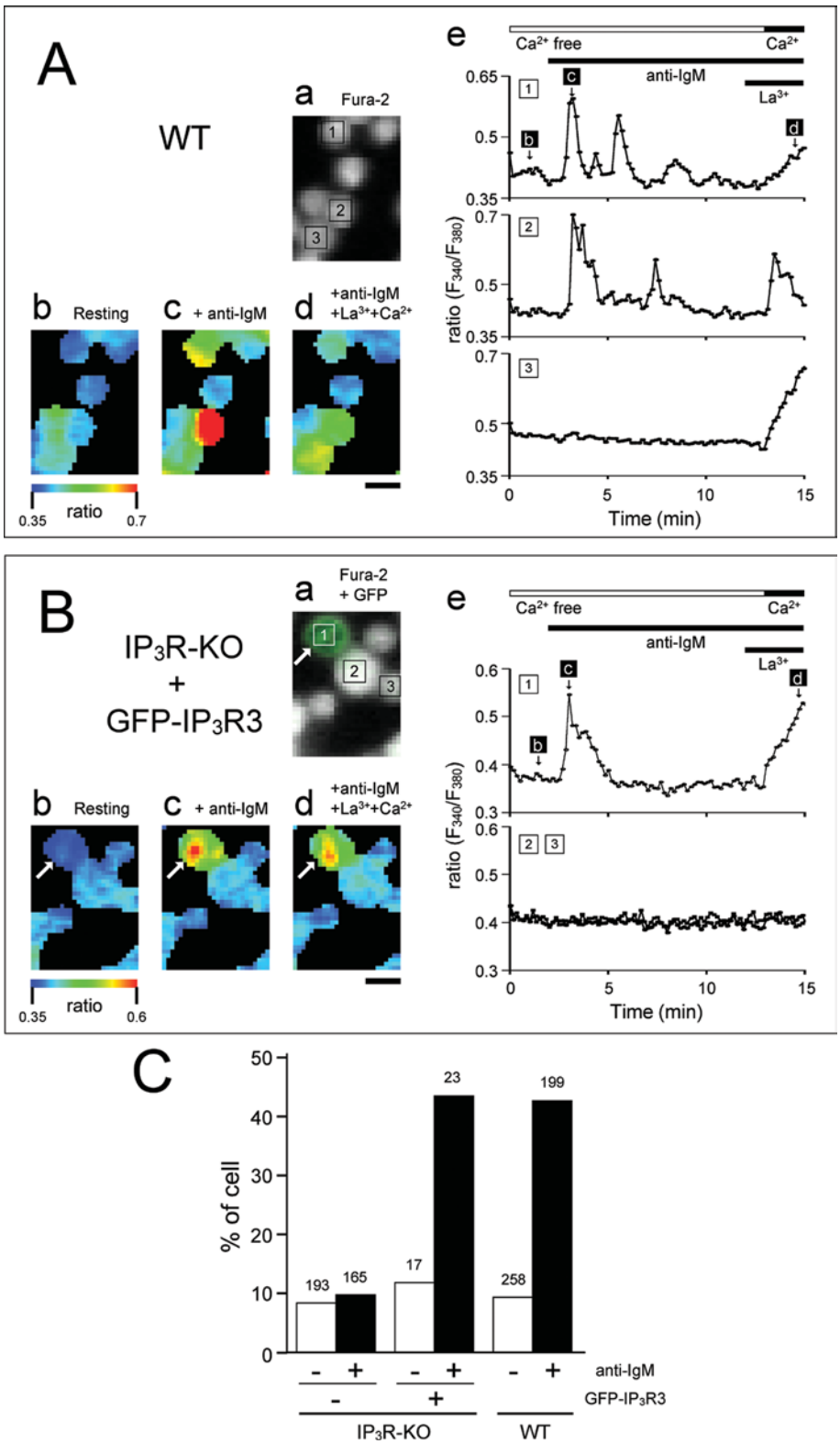

Figure 5 BCR-mediated Ca^{2+} entry in DT40 cells

WT (**A**) and GFP-IP_3R3-transfected IP_3R-KO (**B**) cells were stimulated with anti-IgM in nominally Ca^{2+}-free medium, and La^{3+} (0.3 μM) and Ca^{2+} (1.3 mM) were subsequently added. (**A**) (a) Fluorescence image of fura 2; (b–d) pseudocolour images of fura 2 ratio obtained at time points indicated in (e); (e) time-dependent changes in the fluorescence ratio in the cells depicted in the fluorescence image (a). (**B**) (a) Merged fluorescence image of GFP-IP_3R3 and fura 2; (b–d) pseudocolour images of fura 2 ratio obtained at time points indicated in (e); (e) time-dependent changes in the fluorescence ratio in the cells depicted in the fluorescence image (a). GFP-IP_3R3-expressing cell is indicated by an arrow. The horizontal bars at the top of the Figure indicate the presence of anti-IgM, La^{3+} and Ca^{2+}. The ratio is presented as relative fluorescence intensity (F_{340}/F_{380}). Scale bar, 10 μm. (**C**) La^{3+}-insensitive Ca^{2+} entry was monitored in WT-DT40 cells and GFP-IP_3R3-transfected IP_3R-KO cells. The number of cells showing La^{3+}-insensitive Ca^{2+} entry in the absence (−) and presence (+) of anti-IgM was quantified and plotted as a percentage of the total number of cells. Total number of cells counted is shown above each column.

Expression of IP_3R1 and IP_3R2 was also observed in WT DT40 cells, but not in IP_3R-KO cells, confirming that no IP_3R subtypes were expressed in IP_3R-KO cells (results not shown).

Subcellular localization of GFP-IP_3R3 in DT40 cells

The subcellular distribution of GFP-IP_3R3 was analysed by confocal microscopy (Figure 2). When GFP-IP_3R3 was expressed in IP_3R-KO cells, its fluorescence largely overlapped with the distribution of the ER (Figure 2C). However, a portion of GFP-IP_3R3 appeared to be distinct from the ER distribution and apparently overlapped with the plasma membrane (Figures 2F and 2G). Thus we anticipate that GFP-IP_3R3 serves as a Ca^{2+} channel not only on the ER but also on the plasma membrane.

Luminal Ca^{2+} monitoring

To determine whether GFP-IP_3R3 serves as a functional Ca^{2+} channel on internal Ca^{2+} stores, we monitored IP_3-induced changes in $[Ca^{2+}]_L$ in permeabilized cells. As we have described previously [16], mag-fura 2 was compartmentalized within Ca^{2+} stores in saponin-permeabilized cells, and its fluorescence ratio (343/380 nm) rapidly decreased following the application of 1 μM IP_3, reflecting the IP_3-induced decrease in $[Ca^{2+}]_L$.

This decreased ratio recovered within 5 min of IP_3 removal, reflecting the re-uptake of Ca^{2+} by sarcoplasmic/ER Ca^{2+}-ATPase. IP_3-dependent changes in fluorescence ratio were observed in most WT DT40 cells (21 of 27 cells), but not in IP_3R-KO cells ($n = 49$), confirming the lack of an IP_3-mediated Ca^{2+} release pathway in IP_3R-KO cells (Figures 3A and 3B). The expression of GFP-IP_3R3 restored the IP_3-induced Ca^{2+} release in IP_3R-KO cells (10 of 15 cells, Figure 3B). These results clearly indicate that GFP-IP_3R3 acts as an IP_3-sensitive Ca^{2+} channel.

We then examined the concentration–response relationship for IP_3 on Ca^{2+} release in permeabilized GFP-IP_3R3-expressing cells, and compared it with that in A431 cells, which predominantly expressed IP_3R3 [10]. The time taken for a 50% decrease in the fluorescence ratio became shorter as the IP_3 concentration increased [Figures 3C(a) and 3C(b)]. The concentration–response curve for the estimated IP_3R activity of GFP-IP_3R3 was similar to that of WT IP_3R3 [Figure 3C(c)].

GFP-IP_3R3 function in intact cells

We next examined the function of GFP-IP_3R3 in intact cells. The DT40 cell has an αIgM isotype BCR, which, through activation of PLC (phospholipase C)-γ, mediates an increase in $[Ca^{2+}]_i$ [17,18]. Figure 4(A) shows typical responses of WT DT40 cells to activation of BCR by anti-chicken IgM (anti-IgM, 5 μg/ml). Activation of BCR induced Ca^{2+} responses in 75% of WT cells tested ($n = 95$). The anti-IgM-induced Ca^{2+} responses observed included Ca^{2+} oscillations (48 cells) and monophasic Ca^{2+} transient (20 cells). We also found that trypsin (20 units/ml), an agonist of PAR2 (protease-activated receptor 2), induced transient or oscillatory Ca^{2+} increases in most WT DT40 cells (93 of 96 cells, Figure 4A).

In 17 of the GFP-IP_3R3-expressing cells examined, anti-IgM induced oscillatory (6 cells), monophasic and transient (5 cells) or gradual (1 cell) increases in $[Ca^{2+}]_i$ (Figure 4B). Trypsin also induced Ca^{2+} responses in most of these cells (16 of 17 cells, Figure 4B). When GFP-IP_3R3 was not expressed in IP_3R-KO cells, anti-IgM and trypsin did not induce Ca^{2+} responses (Figure 4B). Anti-IgM-induced Ca^{2+} responses in GFP-IP_3R3-expressing DT40 cells were also observed in the absence of extracellular Ca^{2+}, indicating that GFP-IP_3R3 mediates Ca^{2+} release from internal stores (Figure 4C).

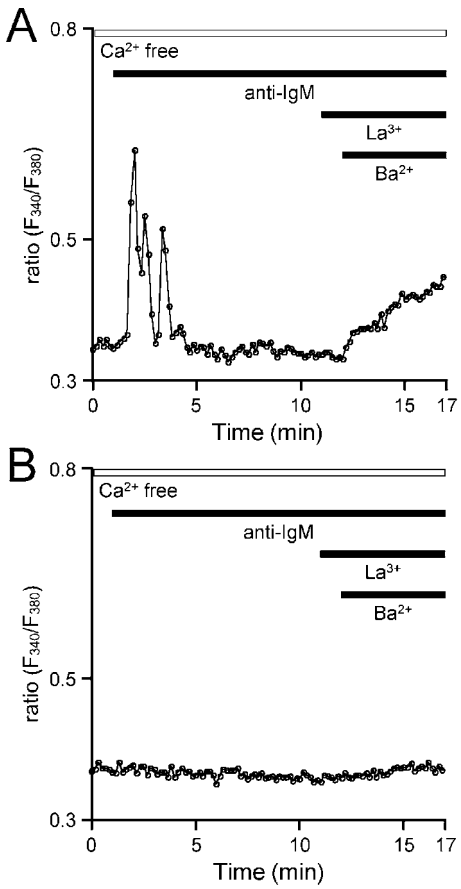

Figure 6 BCR-mediated Ba^{2+} entry

GFP-IP_3R3-expressed IP_3R-KO (**A**) and IP_3R-KO (**B**) cells were stimulated with anti-IgM in nominally Ca^{2+}-free medium and La^{3+} (0.3 μM) and Ba^{2+} (10 mM) were subsequently added. The horizontal bars at the top of the Figure indicate the presence of anti-IgM, La^{3+} and Ba^{2+}. The ratio is presented as relative fluorescence intensity (F_{340}/F_{380}).

BCR-stimulated Ca^{2+} entry requires IP_3R

We next examined the involvement of IP_3R and/or GFP-IP_3R3 in Ca^{2+} entry. BCR-mediated Ca^{2+} responses in WT DT40 cells ceased within 10 min in the absence of extracellular Ca^{2+} (48 of 64 cells). Subsequent increases in external Ca^{2+} led to Ca^{2+} entry, and thus increased $[Ca^{2+}]_i$ in approx. 50% of cells examined (Figures 5A and 5C). Note that this increase in Ca^{2+} concentration occurred in the presence of 0.3 μM La^{3+}, the store-operated channel blocker. BCR-mediated Ca^{2+} entry was also observed in the presence of 1 μM La^{3+} or 1 μM Gd^{3+} (results not shown). In the absence of anti-IgM, La^{3+}-insensitive Ca^{2+} entry was observed in < 10% of cells examined (24 of 258 cells, Figure 5C). Thus it appears that the activation of BCR mediates Ca^{2+} entry in a manner that is distinct from the capacitative pathway, which is activated in response to the depletion of intracellular stores. BCR-mediated La^{3+}-insensitive Ca^{2+} entry was not observed in IP_3R-KO cells, and was restored in approx. 50% of GFP-IP_3R3-expressing IP_3R-KO cells (Figures 5B and 5C). Similarly, activation of BCR stimulated La^{3+}-insensitive Ba^{2+} entry in GFP-IP_3R3-expressing cells (Figure 6). These results indicate that IP_3R or GFP-IP_3R3 is required for BCR-mediated cation entry into DT40 cells.

In contrast, ThG (thapsigargin) caused a transient increase in $[Ca^{2+}]_i$ and depleted Ca^{2+} stores in the absence of extracellular

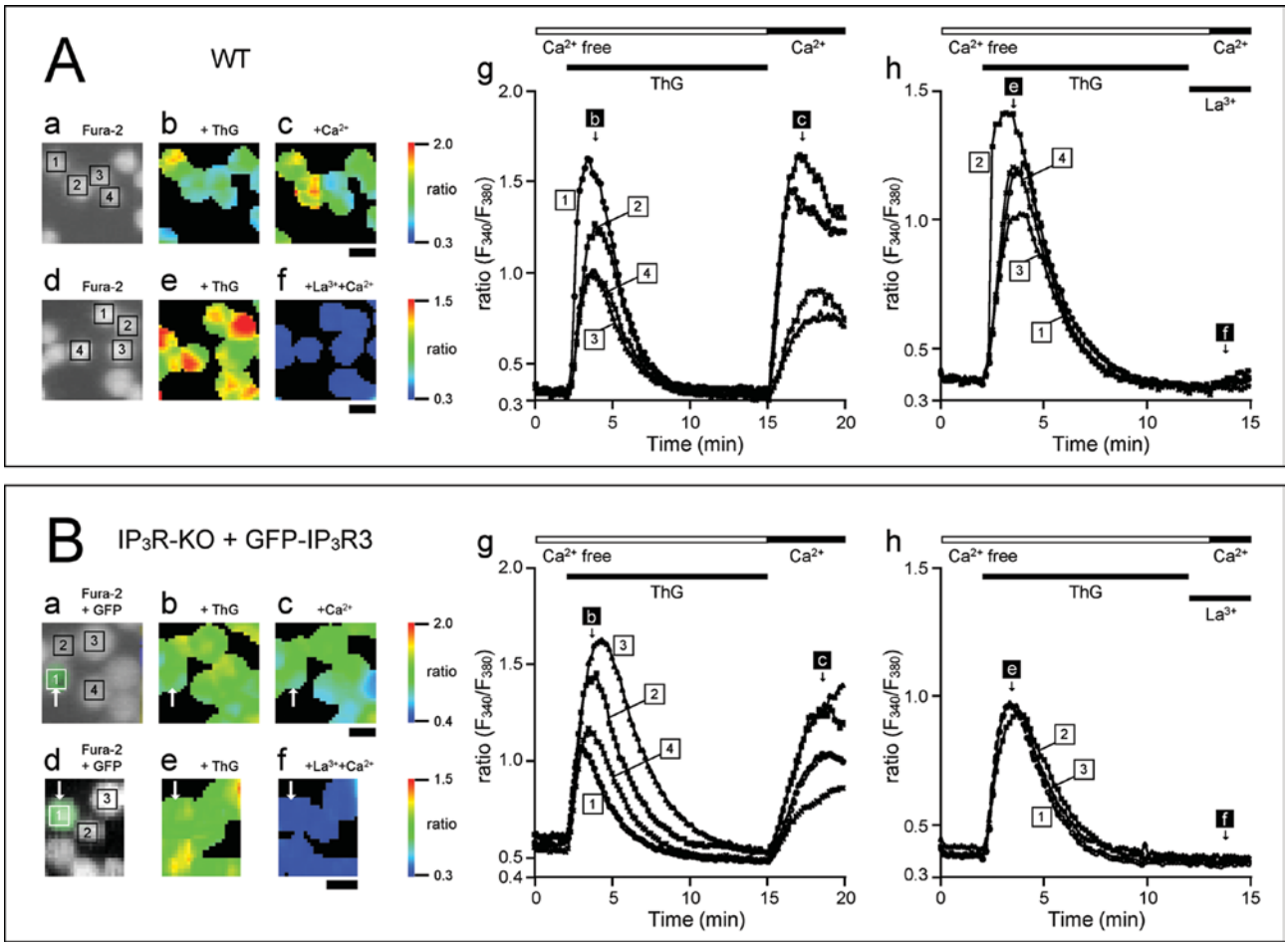

Figure 7 Capacitative Ca^{2+} entry in DT40 cells

WT (**A**) and GFP-IP_3R3-transfected IP_3R-KO (**B**) cells were stimulated with ThG (1 μM) in nominally Ca^{2+}-free medium, and Ca^{2+} (1.3 mM) was subsequently added to the medium in the presence (d–f, h) or absence (a–c, g) of La^{3+}. (**A**) (a, d) Fluorescence image of fura 2; (b, c, e, f) pseudocolour images of fura 2 ratio obtained at time points indicated in (g, h); (g, h) time-dependent changes in the fluorescence ratio in the cells depicted in the fluorescence image (a, d). (**B**) (a, d) Merged fluorescence image of GFP-IP_3R3 and fura 2; (b, c, e, f) pseudocolour images of fura 2 ratio obtained at time points indicated in (g, h); (g, h) time-dependent changes in the fluorescence ratio in the cells depicted in the fluorescence image (a, d). A GFP-IP_3R3-expressing cell is indicated by an arrow. The horizontal bars at the top of the Figure indicate the presence of ThG, La^{3+} and Ca^{2+}. The ratio is presented in terms of relative fluorescence intensity (F_{340}/F_{380}). Scale bar, 10 μm.

Ca^{2+}. Subsequent addition of extracellular Ca^{2+} increased $[Ca^{2+}]_i$ through capacitative Ca^{2+} entry in WT-DT40 cells (Figure 7A). This capacitative Ca^{2+} entry was also observed in IP_3R-KO cells, irrespective of their GFP-IP_3R3 expression state, indicating that IP_3Rs or GFP-IP_3R3 are not essential for capacitative Ca^{2+} entry (Figure 7B). In contrast with BCR stimulation, ThG-induced Ca^{2+} entry was completely blocked by 0.3 μM La^{3+}. These results support the idea that BCR-induced Ca^{2+} entry is not mediated by the depletion of Ca^{2+} stores.

DISCUSSION

We have demonstrated in the present study that the direct application of IP_3 to saponin-permeabilized DT40 cells caused a rapid release of Ca^{2+}. This IP_3-induced Ca^{2+} release was not detected in IP_3R-KO cells, but was restored by the expression of GFP-IP_3R3. In addition, GFP-IP_3R3 showed similar IP_3 sensitivity to that of WT IP_3R3.

The function of GFP-IP_3R3 was also confirmed in intact cells. The M-4 clone of anti-chicken IgM (anti-IgM) is known to stimulate BCR and induce the production of IP_3 via phosphorylation of PLC-γ [15,19]. In addition, trypsin is known to activate PAR2, which is coupled with Gq/11 and induces the production of IP_3 via activation of PLC-β. Both these stimulatory treatments increased $[Ca^{2+}]_i$ in WT, but not in IP_3R-KO, cells. The expression of GFP-IP_3R3 restored the Ca^{2+} response in IP_3R-KO cells. Taken together, these results established that GFP-IP_3R3 serves as a functional IP_3-sensitive Ca^{2+} release channel.

Anti-IgM induced oscillatory Ca^{2+} responses in GFP-IP_3R3-expressing IP_3R-KO cells. A similar oscillatory response has been reported in IP_3R-KO DT40 cells expressing native rat IP_3R3 [20]. It is generally accepted that the oscillatory Ca^{2+} response requires biphasic feedback control by cytoplasmic Ca^{2+}. The activity of IP_3R1 is potentiated at low concentrations of Ca^{2+} (up to 300 nM) and is attenuated at higher concentrations [21]. Similar biphasic control has also been reported for IP_3R3 [22], whereas previously it has been reported that IP_3R3 is not inhibited by high concentrations of cytoplasmic Ca^{2+} [23,24]. Thus the mechanisms of Ca^{2+} oscillation and the role of Ca^{2+} in regulating the function of IP_3R3 are still controversial. GFP-IP_3R3 could become a useful tool for elucidating these issues.

In addition to the well-established role of IP_3Rs as a Ca^{2+} release channel on intracellular organelles, there is also evidence suggesting the involvement of IP_3Rs in Ca^{2+} entry into the cell. This hypothesis, termed the conformational-coupling model,

proposes that a conformational change in IP_3R, caused by store depletion, mediates store-operated channel opening [25]. However, the present study, as well as several other recent studies, demonstrated that capacitative Ca^{2+} entry occurs in IP_3R-KO DT40 cells [15,19,26]. These results strongly indicate that IP_3R is not required for capacitative Ca^{2+} entry, at least in DT40 cells.

In the present study, La^{3+}, a blocker of capacitative Ca^{2+} entry, inhibited ThG-induced Ca^{2+} entry but did not affect BCR-mediated Ca^{2+} entry. This indicated that BCR mediates Ca^{2+} entry via mechanisms that are distinct from capacitative Ca^{2+} entry. In addition, this result is consistent with the observation that BCR mediates the activation of Ba^{2+}-permeable channels [20]. It is considered that the Ba^{2+} entry pathway differs from capacitative Ca^{2+} entry in that Ba^{2+} entry is not caused by the depletion of stores. Both BCR-mediated Ca^{2+} entry and Ba^{2+} entry require IP_3Rs, since they occur in WT DT40 cells but not in IP_3R-KO cells. Moreover, GFP-IP_3R3 was capable of compensating for native IP_3R in BCR-mediated Ca^{2+} entry.

The role(s) of IP_3Rs in controlling Ca^{2+} entry is not known. It is possible that IP_3R and GFP-IP_3R3 themselves are channels for cation entry or that they regulate other channels located on the plasma membrane. In the present study, a portion of GFP-IP_3R3 fluorescence apparently overlapped with that of the plasma membrane, implying that some GFP-IP_3R3 is localized to the plasma membrane. There is also evidence that IP_3R is integrated to the plasma membrane [10]. In addition, several reports have demonstrated that functional IP_3Rs are located on the plasma membrane [11,27]. These lines of evidence suggest that IP_3Rs act as Ca^{2+} entry channels on the plasma membrane.

Several recent studies have suggested that IP_3Rs may migrate. It is suggested in Madin–Darby canine kidney cells that IP_3R1 and IP_3R3 are translocated to the membrane from the cytoplasm during cell polarization [12,13]. Furthermore, in T-lymphocyte Jurkat cells, capping of the T-cell receptor–CD3 complex induces the accumulation of IP_3R to the cap region, which leads to Ca^{2+} entry from that region [6]. Since the distribution of IP_3Rs significantly affects Ca^{2+} signalling, it is predicted that GFP-IP_3R3 will be a useful tool for elucidating the translocation of IP_3R and associated Ca^{2+} responses in living cells.

This study was partially supported by the Academic Sciences Frontier Project and by the Grant-in-Aid for Scientific Research (13771101 to T. M., 14571770 to A. T. and 15591975 to Y. T.) from the Ministry of Education, Culture, Sports, Science and Technology of Japan.

REFERENCES

1 Berridge, M. J. (1993) Inositol trisphosphate and calcium signaling. Nature (London) **361**, 315–325

2 Pozzan, T., Rizzuto, R., Volpe, P. and Meldolesi, J. (1994) Molecular and cellular physiology of intracellular calcium stores. Physiol. Rev. **74**, 595–636

3 Nathanson, M. H., Fallon, M. B., Padfield, P. J. and Maranto, A. R. (1994) Localization of the type 3 inositol 1,4,5-trisphosphate receptor in the Ca^{2+} wave trigger zone of pancreatic acinar cells. J. Biol. Chem. **269**, 4693–4696

4 Lee, M. G., Xu, X., Zeng, W., Diaz, J., Wojcikiewicz, R. J. H., Kuo, T. H., Wuytack, F., Racymaekers, L. and Muallem, S. (1997) Polarized expression of Ca^{2+} channels in pancreatic and salivary gland cells: correlation with initiation and propagation of $[Ca^{2+}]_i$ waves. J. Biol. Chem. **272**, 15765–15770

5 Nezu, A., Tanimura, A., Morita, T., Irie, K., Yajima, T. and Tojyo, Y. (2002) Evidence that zymogen granules do not function as an intracellular Ca^{2+} store for the generation of the Ca^{2+} signal in rat parotid acinar cells. Biochem. J. **363**, 59–66

6 Khan, A. A., Steiner, J. P., Klein, M. G., Schneider, M. F. and Snyder, S. H. (1992) IP_3 receptor: localization to plasma membrane of T cells and cocapping with the T cell receptor. Science **257**, 815–818

7 Fadool, D. A. and Ache, B. W. (1994) Inositol 1,3,4,5-tetrakisphosphate-gated channels interact with inositol 1,4,5-trisphosphate-gated channels in olfactory receptor neurons. Proc. Natl. Acad. Sci. U.S.A. **91**, 9471–9475

8 DeLisle, S., Blondel, O., Longo, F. J., Schnabel, W. E., Bell, G. I. and Welsh, M. J. (1996) Expression of inositol 1,4,5-trisphosphate receptors changes the Ca^{2+} signal of *Xenopus* oocytes. Am. J. Physiol. **270**, C1255–C1261

9 Khan, A. A., Soloski, M. J., Sharp, A. H., Schilling, G., Sabatini, D. M., Li, S.-H., Ross, C. A. and Snyder, S. H. (1996) Lymphocyte apoptosis: mediation by increased type 3 inositol 1,4,5-trisphosphate receptor. Science **273**, 503–507

10 Tanimura, A., Tojyo, Y. and Turner, R. J. (2000) Evidence that type I, II, and III inositol 1,4,5-trisphosphate receptors can occur as integral plasma membrane proteins. J. Biol. Chem. **275**, 27488–27493

11 Kuno, M. and Gardner, P. (1987) Ion channels activated by inositol 1,4,5-trisphosphate in plasma membrane of human T-lymphocytes. Nature (London) **326**, 301–304

12 Colosetti, P., Tunwell, R. E. A., Cruttwell, C., Arsanto, J.-P., Mauger, J.-P. and Cassio, D. (2003) The type 3 inositol 1,4,5-trisphosphate receptor is concentrated at the tight junction level in polarized MDCK cells. J. Cell Sci. **116**, 2791–2803

13 Zhang, S., Mizutani, A., Hisatsune, C., Higo, T., Bannai, H., Nakayama, T., Hattori, M. and Mikoshiba, K. (2003) Protein 4.1N is required for translocation of inositol 1,4,5-trisphosphate receptor type 1 to the basolateral membrane domain in polarized Madin–Darby Canine Kidney cells. J. Biol. Chem. **278**, 4048–4056

14 Morita, T., Tanimura, A., Nezu, A. and Tojyo, Y. (2002) Visualization of inositol 1,4,5-trisphosphate receptor type III with green fluorescent protein in living cells. Cell Calcium **31**, 59–64

15 Sugawara, H., Kurosaki, M., Takata, M. and Kurosaki, T. (1997) Genetic evidence for involvement of type 1, type 2 and type 3 inositol 1,4,5-trisphosphate receptors in signal transduction through the B-cell antigen receptor. EMBO J. **16**, 3078–3088

16 Tanimura, A., Tojyo, Y. and Matsumoto, Y. (1998) Imaging of quantal calcium release in the inositol 1,4,5-trisphosphate-sensitive organelles of permeabilized HSY cells. Cell Struct. Funct. **23**, 129–135

17 Takata, M., Sabe, H., Hata, A., Inazu, T., Homma, Y., Nukada, T., Yamamura, H. and Kurosaki, T. (1994) Tyrosine kinases Lyn and Syk regulate B cell receptor-coupled Ca^{2+} mobilization through distinct pathways. EMBO J. **13**, 1341–1349

18 Takata, M., Homma, Y. and Kurosaki, T. (1995) Requirement of phospholipase C-γ2 activation in surface immunoglobulin M-induced B cell apoptosis. J. Exp. Med. **182**, 907–914

19 Venkatachalam, K., Ma, H.-T., Ford, D. L. and Gill, D. L. (2001) Expression of functional receptor-coupled TRPC3 channels in DT40 triple receptor $InsP_3$ knockout cells. J. Biol. Chem. **276**, 33980–33985

20 Vazquez, G., Wedel, B. J., Bird, G. St. J., Joseph, S. K. and Putney, Jr, J. W. (2002) An inositol 1,4,5-trisphosphate receptor-dependent cation entry pathway in DT40 B lymphocytes. EMBO J. **21**, 4531–4538

21 Bezprozvanny, I., Watras, J. and Ehrlich, B. E. (1991) Bell-shaped calcium-response curves of $Ins(1,4,5)P_3$- and calcium-gated channels from endoplasmic reticulum of cerebellum. Nature (London) **351**, 751–754

22 Cardy, T. J. A., Traynor, D. and Taylor, C. W. (1997) Differential regulation of types-1 and -3 inositol trisphosphate receptors by cytosolic Ca^{2+}. Biochem. J. **328**, 785–793

23 Yoneshima, H., Miyawaki, A., Michikawa, T., Furuichi, T. and Mikoshiba, K. (1997) Ca^{2+} differentially regulates the ligand-affinity states of type 1 and type 3 inositol 1,4,5-trisphosphate receptors. Biochem. J. **322**, 591–596

24 Hagar, R. E., Burgstahler, A. D., Nathanson, M. H. and Ehrlich, B. E. (1998) Type III $InsP_3$ receptor channel stays open in the presence of increased calcium. Nature (London) **396**, 81–84

25 Ma, H.-T., Patterson, R. L., van Rossum, D. B., Birnbaumer, L., Mikoshiba, K. and Gill, D. L. (2000) Requirement of the inositol trisphosphate receptor for activation of store-operated Ca^{2+} channels. Science **287**, 1647–1651

26 Broad, L. M., Braun, F.-J., Lievremont, J.-P., Bird, G. St. J., Kurosaki, T. and Putney, Jr, J. W. (2001) Role of the phospholipase C-inositol 1,4,5-trisphosphate pathway in calcium release-activated calcium current and capacitative calcium entry. J. Biol. Chem. **276**, 15945–15952

27 Lockwich, T. P., Liu, X., Singh, B. B., Jadlowiec, J., Weiland, S. and Ambudkar, I. S. (2000) Assembly of trp1 in a signaling complex associated with caveolin-scaffolding lipid raft domains. J. Biol. Chem. **275**, 11934–11942

Received 23 December 2003/14 May 2004; accepted 3 June 2004
Published as BJ Immediate Publication 3 June 2004, DOI 10.1042/BJ20031970